Binding to the Low-Density Lipoprotein Receptor Accelerates Futile Catalytic Cycling in PCSK9 and Raises the Equilibrium Level of Intramolecular Acylenzyme

Kieran F. Geoghegan,* Lise R. Hoth, Alison H. Varghese, Wen Lin, James G. Boyd, and Matthew C. Griffor

Pfizer Global Research and Development, Groton, Connecticut 06340

Received December 6, 2008; Revised Manuscript Received February 13, 2009

ABSTRACT: Proprotein convertase subtilisin-kexin type 9 (PCSK9) binds to the low-density lipoprotein receptor (LDLR) on target cells and lowers the level of receptor by impeding its recycling. PCSK9 is self-processed to a complex of its prodomain and catalytic domain like a typical protein convertase, but it does not develop normal proteolytic activity. Instead, its propeptide remains complexed with the catalytic domain, and the C-terminal Gln152 of the prodomain occupies the active site like a substrate for peptide synthesis. To probe its latent catalytic activity, PCSK9 and its complex with the soluble LDLR extracellular domain were separately transferred into $H_2{}^{18}O$, and time point samples were analyzed by peptide mapping with mass spectrometry to measure the rate and extent of incorporation of ^{18}O into the Gln152 carboxylate. In free wild-type or D374Y mutant PCSK9, the $t_{1/2}$ for exchange of ^{18}O for both oxygens was near 5 min. This slow process progressed to completion, with the distribution of oxygen isotopes in the Gln152 carboxylate finally matching that in solvent. In contrast, exchange reached its final state in <30 s in LDLR-complexed D374Y mutant PCSK9, but ~40% of the molecules gave data indicating the presence of only one ^{18}O atom in Gln152. With support from further experiments, this was attributed to hydrolysis of acylenzyme in $H_2{}^{16}O$ during preparations for digestion and indicated that PCSK9 complexed with LDLR contains ~40% intramolecular acylenzyme at equilibrium. The synthetic EGF-A domain of LDLR induced similar effects as the full-length receptor. The data suggest the existence of distinct conformational states in free and receptor-bound PCSK9.

Proprotein convertases are intracellular or pericellular proteinases that catalyze the proteolytic maturation of peptide hormones, generally showing selectivity for cleavage sites at basic motifs (*1, 2*). Proprotein convertase subtilisin-kexin type 9 (PCSK9)[1] is a related protein but surprisingly fails to behave like a typical member of the group (*3, 4*). It belongs with the convertases because of relationships in sequence and domain architecture but has its own distinct molecular functions and biological action (*5, 6*). Human PCSK9 is synthesized as a single-chain 692-residue precursor that (typically for a protein convertase) undergoes self-catalyzed processing at a single site, Gln152-Ser153. Then, instead of having its propeptide cleaved by partner enzymes to unmask a catalytically active subtilase, PCSK9 can pass through the protein secretion pathway and be released from its cell of origin. It is believed to circulate in the blood as a binary complex of the prodomain with the catalytic domain, which forms a continuous polypeptide with the Cys/His-rich domain.

The best-defined function of PCSK9 is its binding to the low-density lipoprotein receptor (LDLR) and internalization with it (*7*−*10*). At least one accessory protein is required for this step (*9*). Interaction with PCSK9 leads to LDLR being unable to be recycled to the cell surface, a process that otherwise is very efficient. PCSK9 therefore acts to lower the level of LDLR on the surfaces of liver cells and those of other tissues (*11*), and this activity tends to raise the level of LDL-associated cholesterol. Because excessive elevation of the LDL cholesterol level is a risk factor for cardiovascular disease, PCSK9 is a potential drug target (*12*). This is reinforced by evidence from population genetics demonstrating the deleterious effects on cardiovascular health of certain gain-of-function mutants of PCSK9, of which the most powerful is the D374Y form, as well as beneficial effects of loss-of-function mutations (*13, 14*). Ample evidence from animal studies concurs with the data from humans (*9, 15*).

Interest in these developments has left little attention to spare for the fact that PCSK9 is a proteinase. It seemed plausible at first that PCSK9 would directly degrade the LDLR (*16*), but this possibility was undercut when it was shown that the active site residue Ser386 could be mutated to alanine without disabling receptor modulation (*17, 18*). Nevertheless, while it can be bypassed in the laboratory, the initial self-processing step cannot be eliminated for the activity of secreted PCSK9. The activity of PCSK9 within its cell of origin might be a different case (*15, 19*).

The question of whether self-processing is a one-time event that leaves PCSK9 devoid of further catalytic potential then arises. This might be so, especially as there is at least one important conformational shift associated with self-cleavage (removal of Ser153 from the active site). It is also reasonable

* To whom correspondence should be addressed. Telephone: (860) 441-3601. Fax: (860) 441-3858. E-mail: kieran.f.geoghegan@pfizer.com.

[1] Abbreviations: PCSK9, proprotein convertase subtilisin-kexin type 9; LDLR, low-density lipoprotein receptor; EGF, epidermal growth factor; LC−MS, liquid chromatography−mass spectrometry; MS/MS, tandem mass spectrometry.

10.1021/bi802232m CCC: $40.75
Published on Web 02/17/2009

to consider whether other biological functions of PCSK9, as yet undiscovered, require it to become a fully active proteinase in the ordinary way, but this would not be worth considering if self-processing terminates all activity.

Crystal structures of PCSK9 (*8, 20, 21*) show that the mature protein keeps its catalytic triad of Ser386, His226, and Asp186 in a spatial arrangement that overlaps that found in an active serine protease, proteinase K. The C-terminal strand of the prodomain occupies the nonprime side of the active site groove, with its final residue, Gln152, lying very close to Ser386. This is precisely the kind of structure found in bacterial subtilisins following autocleavage, although producing it as a stable complex has required mutation of the subtilisins to thioenzymes that autoprocess but do not advance to full activation (*22, 23*). From another perspective, the prodomain C-terminus is bound like a substrate for the reverse reaction, but the local conformation change that removes the newly N-terminal Ser153 from the active site makes it impossible for the reverse reaction to continue (*8*).

In view of this structure, we asked whether the catalytic engine of PCSK9 is switched off or idling. Could the enzyme catalyze the exchange of oxygen atoms between the C-terminal carboxyl group of Gln152 and solvent water? Doing so would require the transient formation of an acylenzyme adduct between that group and the (possibly) catalytically active hydroxyl group of Ser386. Moreover, if the process did occur, would its rate be altered by such functionally relevant events as mutations in the sequence or interaction with the LDLR? The results, one of which was briefly noted in an earlier report (*8*), are presented here.

MATERIALS AND METHODS

Protein Expression and Purification. Wild-type PCSK9 and the D374Y mutant were produced in Chinese hamster ovary cells and characterized as described previously (*8*). The complex of PCSK9 D374Y with a FLAG-tagged extracellular fragment of human LDLR was produced by coexpression of the two proteins in Sf9 cells and purified by two steps of affinity chromatography using the FLAG tag as well as the C-terminal His tag on PCSK9. Briefly, DNA encoding the extracellular domain of the human LDL receptor (Swiss-Prot entry P01130) was cloned in frame into a modified pFastBac expression vector (Invitrogen) to encode a fusion protein composed of a 21-residue signal peptide sequence from honey bee melittin, a subsequent Asp-Pro dipeptide, residues 22−720 of human LDLR, and a C-terminal FLAG tag. LDLR residues Asn515 and Asn657 were mutated to Gln to remove canonical sites for N-linked glycosylation. Signal peptide processing by Sf9 insect cells gave a product with an N-terminal sequence of Asp-Pro, indicating precise removal of the 21-residue signal. A construct expressing residues 1−692 of human PCSK9 (Swiss-Prot entry Q8NBP7) with a D374Y mutation followed by a hexahistidine tag was also made in pFastBac. We coexpressed the LDLR fragment with D374Y PCSK9 by infecting Sf9 cells at a density of 3×10^6 cells/mL with both viruses at MOI = 1.0 and harvesting when the viability was ~85%. The complex was first purified by sequential steps of affinity chromatography on an anti-FLAG antibody (with elution by a FLAG peptide) and Ni^{2+}-Sepharose, with a final step of size-exclusion chromatography performed in 0.025 M Tris, 0.3 M NaCl, and 5 mM β-octyl glucoside (pH 7.5). The final purity was evaluated by SDS−polyacrylamide gel electrophoresis (Figure S1 of the Supporting Information), which showed only bands consistent with the expected polypeptides.

Buffers. $H_2{}^{18}O$ (minimum 97 atom %) was purchased from Sigma (p/n 329878). In the absence of an independent measurement of its extent of isotopic substitution, this product has been used as if it was 100% $H_2{}^{18}O$. To prepare Tris/NaCl buffer, separate 0.02 M solutions of Tris-HCl and Tris base in $H_2{}^{18}O$ were combined in a 2:1 ratio (v/v), and the combined solution was used to dissolve a preweighed quantity of NaCl to a final concentration of 0.3 M. Assuming the pK_a of Tris is 8.1, the buffer solution as prepared was calculated by the Henderson−Hasselbalch equation to have a final pH of 7.8. To prepare Mes buffer (pH 6.1), Mes hemisodium (Sigma) was dissolved in $H_2{}^{18}O$ at a concentration of 0.032 M and used to dissolve NaCl to a final concentration of 0.3 M. Checks with pH indicator sticks (colorpHast 0−14, EMD Chemicals) gave results consistent with the expected value for both buffers.

Synthesis of the EGF-A Domain of LDLR. The sequence of the first EGF-like domain of human LDLR (residues Gly292−Asp332 of the mature receptor lacking the 22-residue signal peptide, otherwise defined as residues Gly314−Asp354 of Swiss-Prot entry P01130) was synthesized with a Gly-Ser leader at the N-terminus. The peptide was assembled on an Applied Biosystems ABI433 peptide synthesizer using a preloaded Fmoc-Asp(tBu) *p*-alkoxybenzyl alcohol (Wang) resin and standard Fmoc amino acids. It was cleaved and deprotected by treatment of 0.5 g of synthesis resin with 10 mL of a TFA/water/phenol/thioanisole/ethanedithiol mixture (82.5:5:5:5:2.5) for 2 h. The mixture was filtered, and the peptide was precipitated by dilution of the filtrate into 50 mL of diethyl ether. The crude peptide salt was collected, dried, and partially purified by reverse phase HPLC using a Waters SunFire C_{18} preparative column (19 mm × 100 mm) at a flow rate of 17 mL/min and a dual solvent gradient from 0 to 30% B over 30 min [solvent A, acetonitrile/water/TFA (5:94.9:0.1); solvent B, 100% acetonitrile]. Fractions were analyzed by LC−MS, and appropriate fractions were pooled to provide the reduced intermediate in 75 mL of HPLC solvent at approximately 50% purity (LC−MS deconvoluted average isotopic mass of 4635.89 Da, expected mass of 4635.16 Da). The product pool was treated with 8.0 mg of cystine dihydrochloride, 32 mg of cysteine, 120 mg of methionine, and 5 mL of 1 M Tris-HCl (pH 8.0) to give final concentrations of 0.3 mM cystine, 3.0 mM cysteine, 10 mM methionine, and 62 mM Tris. The pH was adjusted to 8.0, and the solution was stirred at 4 °C for 24 h, during which time a product with a shorter LC−MS retention time formed with a mass 6 Da below that of the reduced product. Subsequent experiments showed that refolding in the presence of 1 mM $CaCl_2$ was faster but did not increase the yield. The solution was acidified to pH ~4 with neat acetic acid, filtered, and HPLC purified as described above to provide the desired product in approximately 95% purity (LC−MS deconvoluted average isotopic mass of 4629.39 Da, expected mass of 4629.09 Da). The product was lyophilized and stored at −20 °C.

Isotope Exchange Reactions and Tryptic Digestions. Isotope exchange reactions were conducted at 22 °C. Wild-

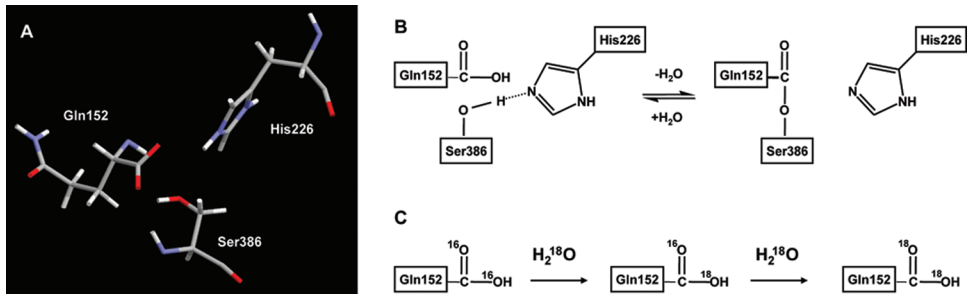

FIGURE 1: (A) Juxtaposition of Gln152, the C-terminal residue of the propeptide of PCSK9, with two residues of the catalytic charge relay system (coordinates provided by X. Qiu, Pfizer Global Research and Development). (B) Futile catalytic cycle envisioned for PCSK9, in which it takes the first step along the reverse catalytic pathway, but the acylenzyme is hydrolyzed to return to the initial state. (C) Hypothetical directional isotope exchange reaction when PCSK9 is diluted into a large excess volume of $H_2{}^{18}O$. This reaction would require the futile catalytic cycle.

type PCSK9 (2.1 mg/mL), PCSK9 D374Y (2.8 mg/mL), or a complex of PCSK9 D374Y with the LDLR extracellular domain (3.5 mg/mL) was diluted 10- or 20-fold into buffered $H_2{}^{18}O$, i.e., final concentrations of 90 or 95% $H_2{}^{18}O$. For the reaction using the EGF-A domain, a solution of the EGF-A domain (0.7 mg/mL, 0.15 mM) was diluted by adding 1 μL of it to 24 μL of Tris-buffered $H_2{}^{18}O$ before PCSK9 D374Y was diluted 20-fold into the mixed solution to start the exchange reaction. Time point samples were withdrawn by pipet and diluted immediately into 8−9 volumes of acetone which was kept at −20 °C until the experiment started. The protein samples in acetone were stored at −20 °C for at least 90 min before protein was collected by centrifugation (2 min at maximum speed in an Eppendorf microfuge). Acetone was removed using a gel loader pipet tip, and the precipitate was dried under vacuum before being redissolved in 0.025 mL of 8 M urea, 0.4 M NH_4HCO_3, and 0.0045 M dithiothreitol. The samples were incubated at 50 °C for 20 min, allowed to cool to 22 °C, and then treated with iodoacetamide at a final concentration of 0.01 M for 20 min. Next, the samples were diluted with water to give a final urea concentration of either 1 or 2 M, and digestion was performed overnight at 37 °C using sequence-grade trypsin (Promega).

As a control experiment, the same chemical protocol was executed with wild-type PCSK9 and its mixture with excess EGF-A precipitated by acetone from 0.02 M Tris-HCl and 0.3 M NaCl (pH 8.0) prepared from standard water, but with all solutions for the postprecipitation workup prepared in $H_2{}^{18}O$. PCSK9 (1.5 mg/mL, 21 μM) or PCSK9 (same concentration) mixed with EGF-A (450 μM) was used in this experiment.

Liquid Chromatography−Mass Spectrometry (LC−MS). For all results in this paper dealing with the rate of isotope exchange, tryptic digests were fractionated on a Vydac C18 column (type 218MS5.510) using a gradient of acetonitrile in 0.1% TFA at a flow rate of 5 μL/min. Mass spectrometry was conducted on a Thermo Fisher LTQ ion trap with standard detectors but operating in Profile mode at Zoom scan rate and with an *m*/*z* 921−934 range to focus on $[M + 2H]^{2+}$ of peptide 137−152 (monoisotopic *m*/*z* 924.9) with continuous collection of isotopic profiles. This method used no data-dependent scans and therefore excluded any inadvertent bias that could have resulted from selection of precursor ions. Digests in early experiments and a final control were also analyzed by standard methods that surveyed all detected signals and allowed collection of the control data on the C-terminal peptide of the catalytic and Cys/His-rich domain.

Software. Calculations of peptide mass values, MS/MS (tandem mass spectrometry) fragmentation, and peptide elementary analyses were performed using version 8.0 of GPMAW (General Protein/Mass Analysis for Windows) (Lighthouse data, Odense, Denmark). Mass spectra of the three isotopic forms of peptide 137−152 of PCSK9 were calculated by entering their respective elementary compositions into the QualBrowser module of Xcalibur version 2.0 (Thermo Fisher) and then exported as *x*−*y* data arrays into Microsoft Excel. Spectral simulations were performed by (i) exporting the experimental spectrum as a graphic to Excel and (ii) using trial and error to calculate a good match between the imported spectrum and a proportional mix of fractional contributions summed to 1.0 of the simulated spectra for the three isotopic forms of peptide 137−152 (details below).

RESULTS

Self-processing of PCSK9 at the Gln152-Ser153 peptide bond appears to be made irreversible by a change in the protein conformation (*8*), leaving Gln152 as a C-terminal residue located close to the catalytic triad residues Ser386 and His226 (Figure 1A). If the reverse reaction could occur, its reaction pathway would begin with formation of an acylenzyme intermediate between Gln152 and Ser386, which would then receive the nucleophilic attack of the α-amino group of Ser153. If the final step never occurs, the alternative is for acylenzyme to be hydrolyzed with delivery of an oxygen atom from solvent into the re-formed carboxyl group of Gln152 (Figure 1B). If this futile catalytic cycle occurred repeatedly, diluting isotopically normal PCSK9 into $H_2{}^{18}O$ would cause directional conversion of the Gln152 carboxyl from its initial all-^{16}O state to an ^{18}O-enriched final state (Figure 1C).

Then 0.02 M Tris-HCl and 0.3 M NaCl (pH 7.8) were prepared in $H_2{}^{18}O$ by dissolving Tris hydrochloride and Tris base at a 2:1 molar ratio in $H_2{}^{18}O$ and dissolving NaCl in the mixed solution. PCSK9 was diluted 10-fold into this buffer at 22 °C to give a protein solution in 90% $H_2{}^{18}O$, and time points were withdrawn by dilution into cold acetone. Enzyme-catalyzed isotope exchange was expected to be terminated by the combined effects of the lower water concentration and protein denaturation by acetone. The

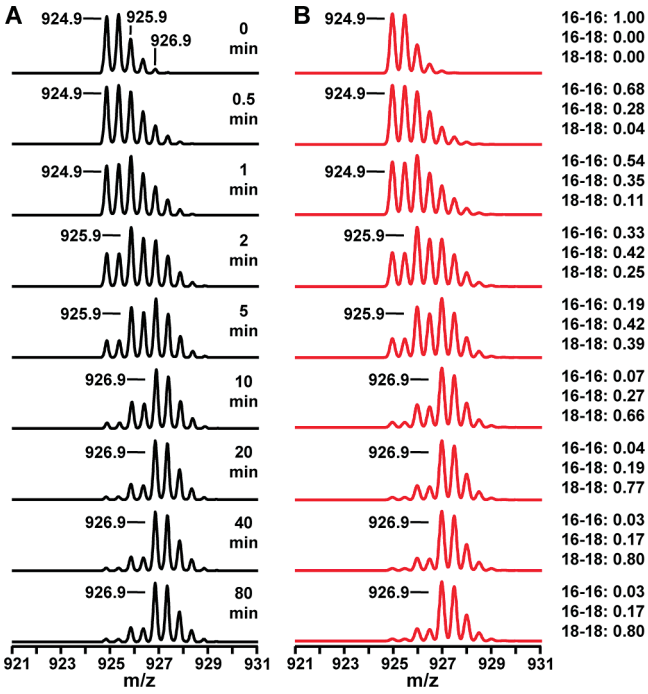

FIGURE 2: (A) Mass spectral peak for $[M + 2H]^{2+}$ of peptide 137−152 of PCSK9 produced by tryptic digestion of protein samples collected from wild-type PCSK9 incubated at 22 °C in Tris-buffered $H_2{}^{18}O$ (pH 7.8). The theoretical monoisotopic *m/z* value for $[M + 2H]^{2+}$ with standard isotopic composition is 924.9. (B) Simulated mass spectra corresponding to the experimental spectra, showing at the right the respective contributions from the forms with two ^{16}O atoms in the Gln152 carboxylate (16−16), one atom each of ^{16}O and ^{18}O (16−18), and two ^{18}O atoms.

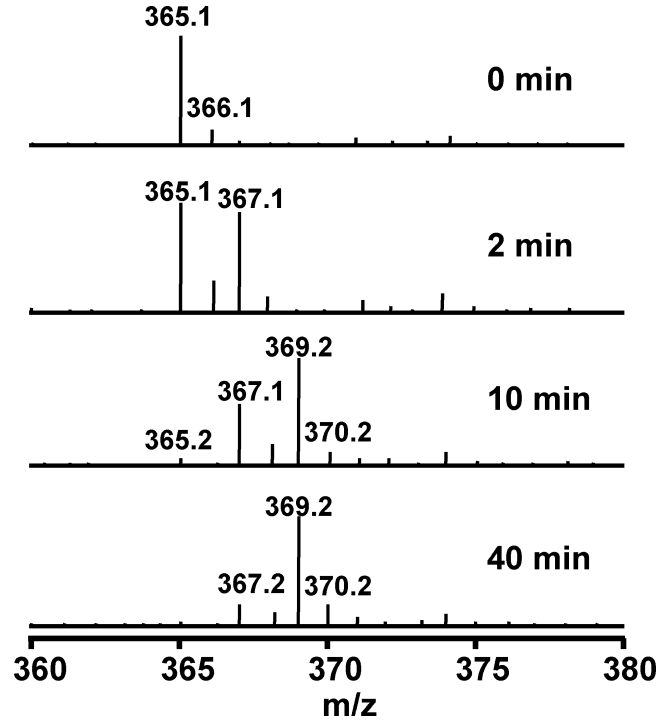

FIGURE 3: Evidence that isotope exchange occurs within the three C-terminal residues of peptide 137−152. Sections of averaged MS/MS spectra from the peak for peptide 137−152 of PCSK9, showing the shift with time of the y_3 ion from *m/z* 365.2 to an intermediate value of *m/z* 367.2 and a final value of *m/z* 369.2.

acetone-treated protein was next pelleted, dried, redissolved in 8 M urea containing 0.4 M NH_4HCO_3 and 4.5 mM dithiothreitol, and incubated at 50 °C for 20 min. After S-alkylation with iodoacetamide and dilution to a nondenaturing concentration of urea, the protein was digested with trypsin and the digests were analyzed by liquid chromatography−mass spectrometry.

Peptide 137−152, the C-terminal tryptic fragment of the prodomain, has a theoretical $[M + 2H]^{2+}$ of 924.9 ($C_{83}H_{121}N_{19}{}^{16}O_{29}$). From a digest of protein that was never in $H_2{}^{18}O$, the isotopic profile of the peptide (Figure 2A, top line) was in good agreement with its theoretical equivalent (Figure 2B, top line). When wild-type PCSK9 was placed in Tris-buffered $H_2{}^{18}O$, peptide 137−152 gradually shifted into species with $[M + 2H]^{2+}$ of 925.9 ($C_{83}H_{121}N_{19}{}^{16}O_{28}{}^{18}O_1$) and $[M + 2H]^{2+}$ of 926.9 ($C_{83}H_{121}N_{19}{}^{16}O_{27}{}^{18}O_2$) (Figure 2A). These shifts in *m/z* for $[M + 2H]^{2+}$ corresponded to mass increases of 2 and 4 Da, respectively, or to the replacement of one and two atoms of ^{16}O with ^{18}O.

Spectral simulation was used to gauge how occupancy of the three isotopic forms of the peptide changed over time (Figure 2B). The mass spectrum was calculated for each isotopic form of the peptide, and combinations at different ratios were evaluated by graphical overlay until each experimental spectrum was acceptably matched. While isotope exchange in free wild-type PCSK9 was slow, it reached a final condition in the 40 and 80 min points in which 80% of peptide 137−152 molecules contained two atoms of ^{18}O. As the buffer was 90% enriched in $H_2{}^{18}O$ after PCSK9 was diluted into it, an 80% population of the two-^{18}O state represented (within experimental error) completion of the isotope exchange process depicted in Figure 1C. This model assumes that the Gln152 carboxylate is nearly completely in the form shown in Figure 1A (i.e., a free carboxylate with two oxygens), implying that the acylenzyme intermediate required for isotope exchange to occur accounts for a very small fraction of PCSK9. This could be consistent with the reaction being relatively slow.

LC−MS gave consistent results for all time points (data not shown), but the mass composition of the 137−152 peptide uniquely changed with time. When MS/MS spectra were compared for this peptide after 0, 2, 10, and 40 min in $H_2{}^{18}O$ (Figure 3), the singly charged y_3 fragment ion derived from the three C-terminal residues shifted from its initial *m/z* value of 365.2 (same as the theoretical value for the all-^{16}O peptide) to a mixed population of forms at *m/z* 365.2, 367.2, and 369.2. The *m/z* 369.2 form became the dominant final form. This was consistent with first one ^{18}O atom (y_3 at *m/z* 367.2) and then a second (y_3 at *m/z* 369.2) being exchanged into Gln152.

While enzyme-catalyzed isotope exchange was anticipated at Gln152, the C-terminal peptide (a histidine tag sequence TGHHHHHH, *m/z* 500.2 for $[M + 2H]^{2+}$) from the Cys/His-rich domain of PCSK9 was also examined as a control. No isotope exchange occurred in this peptide (Figure S2 of the Supporting Information), indicating that exchange was restricted to the special environment of the active site.

The D374Y mutant form of PCSK9 binds ~50 times tighter to the LDLR than the wild type and has correspondingly high biological potency (*7, 8, 24*). To ask whether this remarkably different level of activity might be matched by a faster rate of futile catalysis, PCSK9 D374Y was put through a similar analysis of its isotope exchange behavior in Tris buffer. Graphical comparison of the progress curves

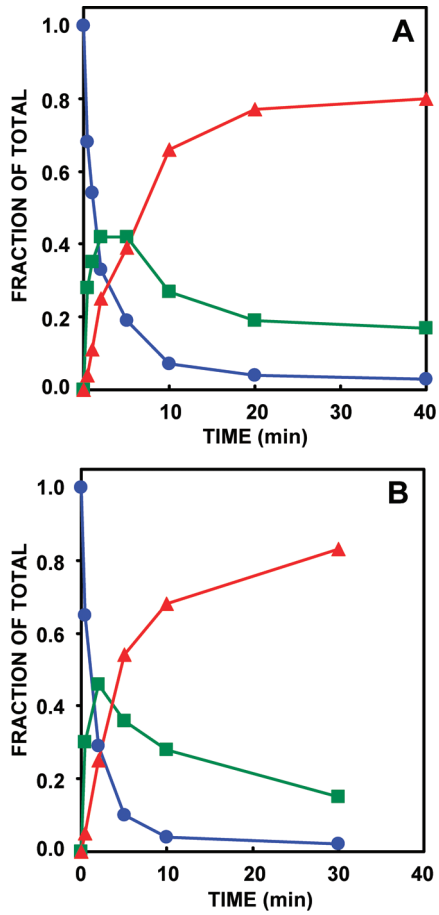

FIGURE 4: Isotope exchange process in peptide 137−152 of (A) wild-type PCSK9 in 90% $H_2{}^{18}O$ and (B) D374Y mutant forms of PCSK9 in 95% $H_2{}^{18}O$: (circles) peptide with two ^{16}O atoms in the Gln152 carboxylate, (squares) peptide with one ^{16}O atom and one ^{18}O atom, and (triangles) peptide with two ^{18}O atoms.

for exchange showed that there was no major difference in the rate of exchange between wild-type and D374Y forms of PCSK9 (Figure 4). As the experiments with the two forms of the protein were performed at different times and used slightly different dilutions in $H_2{}^{18}O$ (exchange was conducted in 90% $H_2{}^{18}O$ for the wild type and 95% $H_2{}^{18}O$ for D374Y), the similarities between the results (discussed in detail below) were much more impressive than any differences, particularly compared to the effects seen in the next experiment.

Biochemical and crystallographic results have shown that PCSK9 interacts with the EGF-A domain of the LDLR (*25*), but it is not certain that this local interaction is the only interaction between the two binding partners. For example, their affinity is higher at the endosomal pH of 5.5 than at or just above neutral pH, and Kwon et al. (*26*) suggested that the structural correlates of this change in affinity may exist in the LDLR rather than in PCSK9. Interaction of PCSK9 with the full receptor could entail a major structural shift in PCSK9, possibly disrupting the interaction of the prodomain with the active site. To probe for such a change, PCSK9 D374Y was coexpressed with a soluble form of the extracellular portion of the LDLR, and the isotope exchange experiment was performed in Tris buffer at pH 7.8 using this protein.

The exchange process for PCSK9 D374Y complexed with the receptor was dramatically different in two ways from that in the free enzyme (Figure 5). First, the process reached

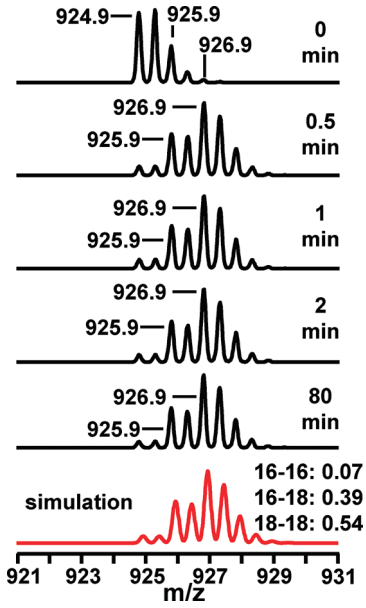

FIGURE 5: Mass spectral peak for $[M + 2H]^{2+}$ of peptide 137−152 of D374Y mutant PCSK9 produced by tryptic digestion of protein samples collected from the PCSK9−LDLR complex incubated at 22 °C in Tris-buffered $H_2{}^{18}O$ (pH 7.8). The spectrum on the last line is the simulated spectrum matching the 30 s and later experimental mass spectra. Other details are as described in the legend of Figure 2.

its final state within 30 s instead of requiring more than 10 min. Second, the final state was quite distinct from that in the free enzyme, with just more than half of the molecules in the $^{18}O-^{18}O$ state in the complex as compared to >80% in free PCSK9. It might be considered that a large percentage of the PCSK9 molecules in the preparation were inactive, but this explanation is ruled out by the fact that the majority of peptide molecules that did not exhibit two-atom exchange are detected with one ^{16}O and one ^{18}O. Inactive molecules would have undergone no exchange and would yield a peptide containing two ^{16}O atoms in the Gln152 carboxylate.

As noted above, PCSK9 interacts with the LDLR at a hot spot located in its EGF-A domain (*25*). We therefore asked whether the EGF-A domain produced by solid-phase chemical synthesis could induce the same change in isotope exchange behavior in PCSK9 as that produced by the entire extracellular sequence. PCSK9 D374Y (final concentration of 2 μM) was added to 0.02 M Tris-buffered $H_2{}^{18}O$ containing the EGF-A domain (final concentration of 5 μM), and the exchange reaction was monitored as described above (Figure 6). Reported affinities between PCSK9 D374Y and an EGF-AB domain fragment (*26*) imply that PCSK9 should be fully complexed with the receptor fragment at the concentrations used in this experiment. With the exception that the first time point was slightly short of the final condition, which could be attributed to the time required for the two molecules to bind to each other, the EGF-A domain produced the same rapid transition to the final state as the full extracellular fragment, and the distribution across isotopic states was also very similar.

The affinity between PCSK9 and LDLR is stronger at lower pH, e.g., at the endosomal pH of 5.5 as compared with pH 7.8, and this work shows that entering the receptor-bound state has strong effects on the futile catalytic cycle of PCSK9. As a lower pH may create a state of PCSK9 with a higher

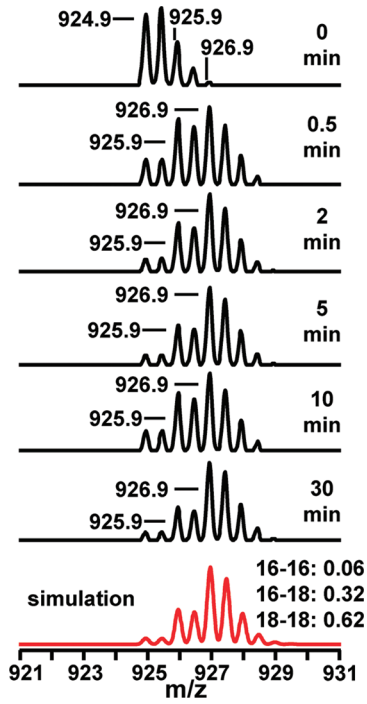

FIGURE 6: Mass spectral peak for $[M + 2H]^{2+}$ of peptide 137−152 of D374Y mutant PCSK9 produced by tryptic digestion of protein samples collected from 2 μM PCSK9 incubated in the presence of 5 μM EGF-A domain produced by peptide synthesis. The complex was incubated at 22 °C in Tris-buffered 95% $H_2{}^{18}O$ (pH 7.8). The spectrum on the last line is the simulated spectrum matching the later spectra from the experiment. Other details are as described in the legend of Figure 2.

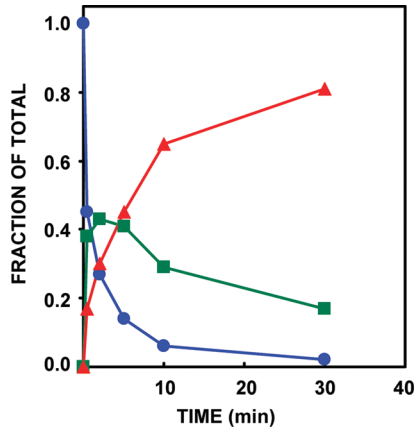

FIGURE 7: Isotope exchange process in peptide 137−152 of D374Y mutant PCSK9 in Mes-buffered 95% $H_2{}^{18}O$ (pH 6.1): (circles) peptide with two ^{16}O atoms in the Gln152 carboxylate, (squares) peptide with one ^{16}O atom and one ^{18}O atom, and (triangles) peptide with two ^{18}O atoms.

affinity for the receptor, we asked whether a pH shift alone would induce part of the functional transition. PCSK9 D374Y was diluted 20-fold into Mes buffer (pH 6.1) in $H_2{}^{18}O$, and oxygen isotope exchange into Gln152 was tested as described above. The process was not appreciably quicker at pH 6.1 than at pH 7.8 (Figure 7).

Finally, as will be discussed in detail below, the distribution between isotopic states in peptide 137−152 complexed with LDLR or its EGF-A domain could be explained by a model in which a substantial fraction of PCSK9 bound to these partners exists as the internal acylenzyme (esterification of the carboxyl group of Gln152 by the hydroxyl group of Ser386). This scheme required that the ester be hydrolyzed during workup of the protein (reduction, S-alkylation, tryptic digestion, and LC−MS), and two distinct experiments were devised to test this explanation.

First, wild-type PCSK9 and its presumed complex with the chemically synthesized EGF-A domain of LDLR were separately acetone-precipitated from 0.02 M Tris-HCl and 0.3 M NaCl (pH 8.0). Supernatants were removed, and the protein pellets were dried. Both samples were then subjected to workup performed entirely in solutions made with $H_2{}^{18}O$ up to the point of injection for LC−MS. From free PCSK9, peptide 137−152 had a normal isotopic envelope, but the same peptide from PCSK9 mixed with EGF-A showed displacement of its isotopic composition in a manner fit reasonably well by the presence of 72% of the peptide having two ^{16}O atoms in the Gln152 carboxylate and 28% of the peptide having one ^{16}O atom and one ^{18}O atom (Figure S3 of the Supporting Information). The heavy oxygen could only have entered the peptide during workup, so the result was consistent with the proposed mechanism. Trypsin-catalyzed insertion was excluded by its failure to occur in PCSK9 precipitated from a solution lacking the EGF-A domain.

Second, to test how the workup conditions affected an ester similar to the one envisioned in PCSK9, L-Tyr-L-Val-L-Phe-L-Ala-L-Gln 2-acetamido-3-oxy-3-aminopropyl ester was subjected to the workup protocol (omitting trypsin) and its stability was evaluated by LC−MS. After the final step, overnight incubation at 37 °C, almost all the ester had been hydrolyzed (Figure S4 of the Supporting Information). Hydrolysis proceeded through two routes: (i) direct hydrolysis to give peptide with C-terminal glutamine and (ii) intramolecular attack by the glutamine side chain amide nitrogen on the ester function with displacement of α-*N*-acetyl-L-serinamide and formation of a cyclic glutarimide, with subsequent ring opening hydrolysis of this intermediate to yield C-terminal glutamine (major product) or isomeric C-terminal glutamic acid amide (trace).

DISCUSSION

For proprotein convertases and subtilases in general, the canonical minimum activation process starts with autocleavage at the end of the prodomain (*27*). This is followed by at least one more proteolytic event in the prodomain, which leads to liberation of the catalytic domain. In eukaryotic cells, different events in this sequence occur in different compartments of the protein secretory apparatus, possibly protecting proteins in early compartments from untimely exposure to proteolysis (*28*). In proprotein convertase PC5A, mutation of the site in the prodomain where the second, intermolecular cleavage event occurs led to the enzyme being secreted as a tight complex of its prodomain with the rest of the enzyme (*29*), exactly the behavior observed with PCSK9. The apparent absence in PCSK9 of an otherwise conserved basic site for the second cut in the prodomain suggests that it has evolved to avoid the normal pathway for discarding its prodomain.

Consistent with this possibility, PCSK9 affects LDLR levels without acting in trans as a protease (*17, 18*). The molecules interact by mutual binding, and their enhanced affinity at endosomal pH diverts the receptor from its usually efficient recycling pathway into a terminal fate (*25*). How-

ever, little is known about the extent or nature of any internal changes that occur in PCSK9 during this process, in the course of which the receptor is thought to undergo a major conformational change (*30*). Comparison of the crystal structures of the free wild-type protein (*8, 20, 21*) and of the D374Y mutant complexed with a EGF-A/B domain fragment of LDLR (*26*) reveals no major domain shifts. In particular, both structures show the C-terminal residue of the propeptide, Gln152, as a discrete residue with two oxygen atoms in its carboxyl group, and located close to but not covalently bound to the active site Ser386 (Figure 1A).

Crystallography generally gives a static image of protein structure, and the fact that the "self-inhibited" structure of PCSK9 can also be viewed as that of an enzyme−substrate complex for the reverse reaction invited speculation that vestigial catalytic function might remain in the form of a futile cycle (Figure 1B). PCSK9 therefore offered an excellent chance to look into the catalytic potential of an autoprocessed subtilase.

Mass analysis of the 137−152 peptide fragment of PCSK9 was used to assess enzyme-catalyzed oxygen isotope exchange. Considering the proximity of Gln152 to Ser386 indicated by crystal structures, the process of enzyme-catalyzed oxygen isotope exchange between the solvent and the carboxyl group of Gln152 that occurred in free PCSK9 (wild-type and D374Y mutant) at pH 7.8 and 22 °C was surprisingly slow (Figures 2−4), proceeding to completion on a time scale of ~20 min. As noted in Results, 80% population of the doubly ^{18}O-labeled state amounted to complete exchange, because the water in the exchange reaction was 90 atom % enriched in ^{18}O, there are two oxygens in the target carboxyl, and the square of 0.90 is 0.81. Tandem MS of the target peptide confirmed that the exchange occurred in that group, as the *m/z* value for the singly charged y_3 ion progressively shifted from its initial *m/z* value of 365 into peaks at *m/z* 367 and 369 in parallel with the mass shift for the intact peptide (Figure 3).

Two important differences were detected when the isotope exchange rate was measured for PCSK9 D374Y complexed with the LDLR extracellular domain. First, the condition measured after 30 s was also the final state of the system (Figure 5), indicating that exchange was much faster in receptor-bound PCSK9. Second, and even more intriguing, the isotope distribution pattern was quite different from the final state in the free protein.

If isotope exchange in PCSK9 bound to LDLR followed the model that accounts for the process in the free enzyme, the proportions of the three isotopic forms expected in peptide 137−152 would be 0% $^{16}O-^{16}O$, 10% $^{16}O-^{18}O$, and 90% $^{18}O-^{18}O$ (dilution in this experiment was to 95 atom % $H_2{}^{18}O$). The observed proportions (Figure 5) differed from these by the following fractional values: $^{16}O-^{16}O$, +7%; $^{16}O-^{18}O$, +29%; $^{18}O-^{18}O$, −36%. Thus, a deficit in doubly exchanged peptide was balanced by a surplus versus theory in the unexchanged and once-exchanged products.

To the best of our knowledge, the only plausible explanation for this result is the fact that ~43% of PCCSK9 D374Y bound to LDLR is in the intramolecular acylenzyme form, in which Gln152 is esterified by Ser386. Hydrolysis of the ester during analytical workup in $H_2{}^{16}O$ would yield the enhanced level of $^{16}O-^{18}O$ peptide (Figure 8).

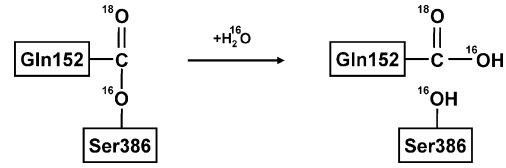

FIGURE 8: Proposed origin of the peptide with one carboxylate oxygen as ^{18}O from PCSK9 complexed with LDLR or the EGF-A domain. Exchange occurs repeatedly and relatively rapidly in the complexed protein, but the fraction of PCSK9 trapped as acylenzyme is hydrolyzed during preparation for digestion and yields a product with one ^{16}O atom and one ^{18}O atom.

The model accounts for the experimental result as follows. From 95 atom % $H_2{}^{18}O$, if a fraction equal to 57% of Gln152 in PCSK9 D374Y is in the form shown in Figure 1A (two free oxygens), this should yield a fraction of 54% of the 137−152 peptide in the $^{18}O-^{18}O$ form and would be the only source of that product (experimental value of 54%). If the remaining fraction (43%) of PCSK9 exists as the acylenzyme, a portion equal to 41% of the total PCSK9 will yield $^{16}O-^{18}O$ peptide 137−152 after hydrolysis during workup (experimental value of 39%). Free and acylenzyme PCSK9 should contribute fractions of 3% and 2%, respectively, to the $^{16}O-^{16}O$ product (total of 5%, experimental value of 7%). Overall, the experimental results are reasonably explained by postulating that ~40% of the PCSK9 exists as acylenzyme when bound to the LDLR extracellular domain, and this explanation was supported by experiments designed to challenge it (Figures S3 and S4 of the Supporting Information).

As the EGF-A domain of LDLR is a contact region for PCSK9 (*25, 26, 31*), we conducted an isotope exchange study in which 5 μM EGF-A domain was mixed with 2 μM PCSK9 D374Y. In a remarkably clear confirmation that the small EGF-A domain delivers a major part, if not all, of the receptor's effect on PCSK9 (*32, 33*), the PCSK9 complexed with this 4.5 kDa polypeptide behaved in essentially the same way as PCSK9 bound to the much larger LDLR extracellular domain (Figure 6), although the implied fraction of PCSK9 in the acylenzyme form was slightly lower.

A limited study was made of the effect of pH on isotope exchange, but no marked acceleration was observed at pH 6.1 compared to pH 7.8. It remains possible that the change in affinity is due to changes (presumably ionizations) that occur in the LDLR (*26*).

None of the crystal structures published for free PCSK9 (*8, 20, 21*) or its complexes with an EGF domain of LDLR (*26, 32*) show any sign of acylenzyme being present. This is easily explained in the case of free PCSK9, for which isotope exchange data show that a non-zero but very low level of acylenzyme must (on average) exist in solution; therefore, the failure of crystallography to detect its existence is not surprising. Even if crystalline PCSK9 can catalyze isotope exchange, which has not been studied, the crystallographic solution will converge on the structure of the majority of molecules.

For receptor-bound PCSK9, the fraction of acylenzyme implied from isotope exchange was ~40%, so the fact that the crystallographic solution for the PCSK9−EGF-AB complex showed two oxygens in the Gln152 carboxylate and no covalent bond to Ser386 requires explanation. The conditions of data collection must influence molecular

dynamics, and crystals are cooled to 90−100 K when diffraction data are collected using a high-intensity X-ray source. This cooling may cause the protein to favor the lowest-energy structure available as opposed to populating all the states occupied in solution at physiological temperatures.

Structural studies show that LDLR (or its relevant fragment, EGF-A) binds to PCSK9 at a site that is remote from the active site; therefore, their action on the futile catalytic cycle in the active site can (loosely) be called allosteric. Although the distinction may be fine at the level of structure, the protein appears to exist either in a free conformation with a lazy catalytic cycle or in a receptor-bound one in which the catalytic cycle runs much faster and the acylenzyme state is much more highly occupied. The EGF-A domain proved to be a good surrogate for the entire LDLR in inducing this shift between states. It is possible that measuring this function of PCSK9, which is only the second catalytic function to be defined and the first that can occur more than once per molecule, can prove to be a useful probe of the effects on PCSK9 of such agents as antibodies, truncation of the N-terminus (*26*), or changes in pH.

Evolution has led PCSK9 to deliver a function quite separate from the one first suggested by its sequence. The existence of this function, however, does not exclude the possibility that PCSK9 could mature as a protease in some other biological context that has not yet been discovered, although the difficulty that we and others had in revealing any proteolytic activity after self-processing suggests that other specialized protein factors could be involved. This work confirms that the catalytic machinery of PCSK9 is viable in the purified, self-processed enzyme and operates with greater efficiency when PCSK9 is bound to LDLR. It follows that unmasking of this activity in an intracellular context remains theoretically possible.

ACKNOWLEDGMENT

We thank Timothy A. Subashi for cell production support.

SUPPORTING INFORMATION AVAILABLE

Four figures depicting the purity of a protein reagent, a control experiment, an experiment that probed the paper's main conclusion from an additional perspective, and a model reaction. This material is available free of charge via the Internet at http://pubs.acs.org.

REFERENCES

1. Seidah, N. G., Mayer, G., Zaid, A., Rousselet, E., Nassoury, N., Poirier, S., Essalmani, R., and Prat, A. (2008) The activation and physiological functions of the proprotein convertases. *Int. J. Biochem. Cell Biol. 40*, 1111–1125.
2. Henrich, S., Lindberg, I., Bode, W., and Than, M. E. (2005) Proprotein convertase models based on the crystal structures of furin and kexin: Explanation of their specificity. *J. Mol. Biol. 345*, 211–227.
3. Attie, A. D. (2004) The mystery of PCSK9. *Arterioscler., Thromb., Vasc. Biol. 24*, 1337–1339.
4. Lopez, D. (2008) PCSK9: An enigmatic protease. *Biochim. Biophys. Acta 1781*, 184–191.
5. Horton, J. D., Cohen, J. C., and Hobbs, H. H. (2007) Molecular biology of PCSK9: Its role in LDL metabolism. *Trends Biochem. Sci. 32*, 71–77.
6. Seidah, N. G., Khatib, A. M., and Prat, A. (2006) The proprotein convertases and their implication in sterol and/or lipid metabolism. *Biol. Chem. 387*, 871–877.
7. Cameron, J., Holla, O. L., Ranheim, T., Kulseth, M. A., Berge, K. E., and Leren, T. P. (2006) Effect of mutations in the PCSK9 gene on the cell surface LDL receptors. *Hum. Mol. Genet. 15*, 1551–1558.
8. Cunningham, D., Danley, D. E., Geoghegan, K. F., Griffor, M. C., Hawkins, J. L., Subashi, T. A., Varghese, A. H., Ammirati, M. J., Culp, J. S., Hoth, L. R., Mansour, M. N., McGrath, K. M., Seddon, A. P., Shenolikar, S., Stutzman-Engwall, K. J., Warren, L. C., Xia, D., and Qiu, X. (2007) Structural and biophysical studies of PCSK9 and its mutants linked to familial hypercholesterolemia. *Nat. Struct. Mol. Biol. 14*, 413–419.
9. Lagace, T. A., Curtis, D. E., Garuti, R., McNutt, M. C., Park, S. W., Prather, H. B., Anderson, N. N., Ho, Y. K., Hammer, R. E., and Horton, J. D. (2006) Secreted PCSK9 decreases the number of LDL receptors in hepatocytes and in livers of parabiotic mice. *J. Clin. Invest. 116*, 2995–3005.
10. Qian, Y.-W., Schmidt, R. J., Zhang, Y., Chu, S., Lin, A., Wang, H., Wang, X., Beyer, T. P., Bensch, W. R., Li, W., Ehsani, M. E., Lu, D., Konrad, R. J., Eacho, P. I., Moller, D. E., Karathanasis, S. K., and Cao, G. (2007) Secreted PCSK9 downregulates low density lipoprotein receptor through receptor-mediated endocytosis. *J. Lipid Res. 48*, 1488–1498.
11. Schmidt, R. J., Beyer, T. P., Bensch, W. R., Qian, Y.-W., Lin, A., Kowala, M., Alborn, W. E., Konrad, R. J., and Cao, G. (2008) Secreted proprotein convertase subtilisin/kexin type 9 reduces both hepatic and extrahepatic low-density lipoprotein receptors in vivo. *Biochem. Biophys. Res. Commun. 370*, 634–640.
12. Costet, P., Krempf, M., and Cariou, B. (2008) PCSK9 and LDL cholesterol: Unravelling the target to design the bullet. *Trends Biochem. Sci. 33*, 426–434.
13. Abifadel, M., Varret, M., Rabes, J.-P., Allard, D., Ouguerram, K., Devillers, M., Cruaud, C., Benjannet, S., Wickham, L., Erlich, D., Derre, A., Villeger, L., Farnier, M., Beucler, I., Bruckert, E., Chambaz, J., Chanu, B., Lecerf, J.-M., Luc, G., Moulin, P., Weissenbach, J., Prat, A., Krempf, M., Junien, C., Seidah, N. G., and Boileau, C. (2003) Mutations in PCSK9 cause autosomal dominant hypercholesterolemia. *Nat. Genet. 34*, 154–156.
14. Cohen, J. C., Boerwinkle, E., Mosley, T. H., Jr., and Hobbs, H. H. (2006) Sequence variations in PCSK9, low LDL, and protection against coronary heart disease. *N. Engl. J. Med. 354*, 1264–1272.
15. Maxwell, K. N., Fisher, E. A., and Breslow, J. L. (2005) Overexpression of PCSK9 accelerates the degradation of the LDLR in a post-endoplasmic reticulum compartment. *Proc. Natl. Acad. Sci. U.S.A. 102*, 2069–2074.
16. Tall, A. R. (2006) Protease variants, LDL, and coronary heart disease. *N. Engl. J. Med. 354*, 1310–1312.
17. Li, J., Tumanut, C., Gavigan, J.-A., Huang, W.-J., Hampton, E. N., Tumanut, R., Suen, K. F., Trauger, J. W., Spraggon, G., Lesley, S. A., Liau, G., Yowe, D., and Harris, J. L. (2007) Secreted PCSK9 promotes LDL receptor degradation independently of proteolytic activity. *Biochem. J. 406*, 203–207.
18. McNutt, M. C., Lagace, T. A., and Horton, J. D. (2007) Catalytic activity is not required for secreted PCSK9 to reduce low density lipoprotein receptors in HepG2 cells. *J. Biol. Chem. 282*, 20799–20803.
19. Nassoury, N., Blasiole, D. A., Oler, A. T., Benjannet, S., Hamelin, J., Poupon, V., McPherson, P. S., Attie, A. D., Prat, A., and Seidah, N. G. (2007) The cellular trafficking of the secretory proprotein convertase PCSK9 and its dependence on the LDLR. *Traffic 8*, 718–732.
20. Piper, D. E., Jackson, S., Liu, Q., Romanow, W. G., Shetterly, S., Thibault, S. T., Shan, B., and Walker, N. P. C. (2007) The crystal structure of PCSK9: A regulator of plasma LDL-cholesterol. *Structure (Cambridge, MA, U.S.) 15*, 545–552.
21. Hampton, E. N., Knuth, M. W., Li, J., Harris, J. L., Lesley, S. A., and Spraggon, G. (2007) The self-inhibited structure of full-length PCSK9 at 1.9 angstrom reveals structural homology with resistin within the C-terminal domain. *Proc. Natl. Acad. Sci. U.S.A. 104*, 14604–14609.
22. Tanaka, S., Matsumura, H., Koga, Y., Takano, K., and Kanaya, S. (2007) Four new crystal structures of Tk-subtilisin in unautoprocessed, autoprocessed and mature forms: Insight into structural changes during maturation. *J. Mol. Biol. 372*, 1055–1069.
23. Jain, S. C., Shinde, U., Li, Y., Inouye, M., and Berman, H. M. (1998) The crystal structure of an autoprocessed Ser221Cys-subtilisin E-propeptide complex at 2.0 angstrom resolution. *J. Mol. Biol. 284*, 137–144.

24. Naoumova, R. P., Tosi, I., Patel, D., Neuwirth, C., Horswell, S. D., Marais, A. D., van Heyningen, C., and Soutar, A. K. (2005) Severe hypercholesterolemia in four British families with the D374Y mutation in the PCSK9 gene. *Arterioscler., Thromb., Vasc. Biol. 25*, 2654–2660.
25. Zhang, D.-W., Lagace, T. A., Garuti, R., Zhao, Z., McDonald, M., Horton, J. D., Cohen, J. C., and Hobbs, H. H. (2007) Binding of proprotein convertase subtilisin/kexin type 9 to epidermal growth factor-like repeat A of low density lipoprotein receptor decreases receptor recycling and increases degradation. *J. Biol. Chem. 282*, 18602–18612.
26. Kwon, H. J., Lagace, T. A., McNutt, M. C., Horton, J. D., and Deisenhofer, J. (2008) Molecular basis for LDL receptor recognition by PCSK9. *Proc. Natl. Acad. Sci. U.S.A. 105*, 1820–1825.
27. Anderson, E. D., VanSlyke, J. K., Thulin, C. D., Jean, F., and Thomas, G. (1997) Activation of the furin endoprotease is a multiple-step process: Requirements for acidification and internal propeptide cleavage. *EMBO J. 16*, 1508–1518.
28. Anderson, E. D., Molloy, S. S., Jean, F., Fei, H., Shimamura, S., and Thomas, G. (2002) The ordered and compartment-specific autoproteolytic removal of the furin intramolecular chaperone is required for enzyme activation. *J. Biol. Chem. 277*, 12879–12890.
29. Nour, N., Basak, A., Chretien, M., and Seidah, N. G. (2003) Structure-function analysis of the prosegment of the proprotein convertase PC5A. *J. Biol. Chem. 278*, 2886–2895.
30. Rudenko, G., Henry, L., Henderson, K., Ichtchenko, K., Brown, M. S., Goldstein, J. L., and Deisenhofer, J. (2002) Structure of the LDL receptor extracellular domain at endosomal pH. *Science 298*, 2353–2358.
31. Shan, L., Pang, L., Zhang, R., Murgolo, N. J., Lan, H., and Hedrick, J. A. (2008) PCSK9 binds to multiple receptors and can be functionally inhibited by an EGF-A peptide. *Biochem. Biophys. Res. Commun. 375*, 69–73.
32. Bottomley, M. J., Cirillo, A., Orsatti, L., Ruggeri, L., Fisher, T. S., Santoro, J. C., Cummings, R. T., Cubbon, R. M., Lo Surdo, P., Calzetta, A., Noto, A., Baysarowich, J., Mattu, M., Talamo, F., De Francesco, R., Sparrow, C. P., Sitlani, A., and Carfi, A. (2009) Structural and biochemical characterization of the wild type PCSK9-EGF(AB) complex and natural familial hypercholesterolemia mutants. *J. Biol. Chem. 284*, 1313–1323.
33. Zhang, D.-W., Garuti, R., Tang, W.-J., Cohen, J. C., and Hobbs, H. H. (2008) Structural requirements for PCSK9-mediated degradation of the low-density lipoprotein receptor. *Proc. Natl. Acad. Sci. U.S.A. 105*, 13045–13050.

BI802232M